

- reached. This approach was used to estimate relative maximum leaf size during the period of study (Fig. 3).
29. The threshold for thermal damage of nonsucculent leaves (45° to 52°C) is a highly conserved characteristic across a wide range of extant taxa [W. Larcher, in *Ecophysiology of Photosynthesis*, E. D. Schultze and M. M. Caldwell, Eds. (Springer-Verlag, Berlin, 1994), pp. 261–277; Y. Gauslaa, *Holarct. Ecol.* **7**, 1 (1984)], implying little evolutionary change through time.
 30. T. A. Mansfield, A. M. Hetherington, C. J. Atkinson, *Annu. Rev. Plant Physiol. Plant Mol. Biol.* **41**, 55 (1990).
 31. A review of fossil Ginkgoalean leaves revealed that species with the most dissected leaves, characterized by multidichotomies 0.5 to 2 mm wide, are restricted to Late Triassic to early Middle Jurassic facies [T. Kimura, G. Naito, T. Ohana, *Bull. Natl. Sci. Mus. Tokyo* **9**, 91 (1983)].
 32. The cause of T-J floral turnover has traditionally been attributed to a sedimentary hiatus (3). However, this hypothesis is unsupported by sedimentological evidence [G. Dam and F. Surlyk, *Geology* **20**, 749 (1992); *Spec. Publ. Int. Assoc. Sedimentol.* **18**, 4189 (1993)], which identifies no major facies changes or conformities between the T-J strata in Greenland. Furthermore, the absence of the upper Rhaetian *Ricciisporites-Polypodisporites* acme zone [W. M. L. Schuurman, *Rev. Palaeobot. Palynol.* **23**, 159 (1977)] in Greenland (10) and Sweden (11), which has also been tentatively interpreted as evidence of a hiatus at both localities, is questionable, as acme zones are generally considered of only local use, owing to the effects of ecological, environmental, and postdepositional processes on relative pollen abundances.
 33. The value of $\delta^{13}\text{C}$ is
- $$\delta^{13}\text{C} = \left[\left(\frac{^{13}\text{C}_{\text{unk}}/^{12}\text{C}_{\text{unk}}}{^{13}\text{C}_{\text{std}}/^{12}\text{C}_{\text{std}}} \right) - 1 \right] \times 1000$$
- where unk the ratio of unknown to sample and std is the ratio of the pee dee belemnite standard.
34. F. M. Grandstein et al., *J. Geophys. Res.* **99**, 24051 (1994).
 35. We thank E. M. Friis (Swedish Museum of Natural History) and S. Funder (Danish Geological Museum) for loans and provision of fossil leaves; P. E. Olsen, F. Surlyk, W. G. Chaloner, D. J. Read, R. A. Spicer, C. K. Kelly, and P. Wignall for comments on earlier versions; and the Isotope Laboratory at Royal Holloway College, University of London, for making measurements of $\delta^{13}\text{C}$. We gratefully acknowledge funding from the Natural Environment Research Council, UK (GR9/O2930), and through Royal Society Research Fellow and Equipment grants to D.J.B.

21 April 1999; accepted 26 July 1999

Gene Expression Profile of Aging and Its Retardation by Caloric Restriction

Cheol-Koo Lee,^{1,3} Roger G. Klopp,²
Richard Weindruch,^{4*} Tomas A. Prolla^{3*}

The gene expression profile of the aging process was analyzed in skeletal muscle of mice. Use of high-density oligonucleotide arrays representing 6347 genes revealed that aging resulted in a differential gene expression pattern indicative of a marked stress response and lower expression of metabolic and biosynthetic genes. Most alterations were either completely or partially prevented by caloric restriction, the only intervention known to retard aging in mammals. Transcriptional patterns of calorie-restricted animals suggest that caloric restriction retards the aging process by causing a metabolic shift toward increased protein turnover and decreased macromolecular damage.

Most multicellular organisms exhibit a progressive and irreversible physiological decline that characterizes senescence, the molecular basis of which remains unknown. Postulated mechanisms include cumulative damage to DNA leading to genomic instability, epigenetic alterations that lead to altered gene expression patterns, telomere shortening in replicative cells, oxidative damage to critical macromolecules by reactive oxygen species (ROS), and nonenzymatic glycation of long-lived proteins (1, 2).

Genetic manipulation of the aging process in multicellular organisms has been achieved in *Drosophila* through the overexpression of

catalase and Cu/Zn superoxide dismutase (3), in the nematode *Caenorhabditis elegans* through alterations in the insulin receptor signaling pathway (4), and through the selection of stress-resistant mutants in either organism (5). In mammals, mutations in the Werner Syndrome locus (WRN) accelerate the onset of a subset of aging-related pathology in humans (6), but the only intervention that appears to slow the intrinsic rate of aging is caloric restriction (CR) (7). Most studies have involved laboratory rodents which, when subjected to a long-term, 25 to 50% reduction in calorie intake without essential nutrient deficiency, display delayed onset of age-associated pathological and physiological changes and extension of maximum lifespan. Postulated mechanisms of action include increased DNA repair capacity, altered gene expression, depressed metabolic rate, and reduced oxidative stress (7).

To examine the molecular events associated with aging in mammals, we used oligonucleotide-based arrays to define the transcriptional response to the aging process in mouse gastrocnemius muscle. Our choice of tissue was guided by the fact that skeletal muscle is primarily composed of long-lived, high oxygen-consuming postmitotic cells, a

feature shared with other critical aging targets such as heart and brain. Loss of muscle mass (sarcopenia) and associated motor dysfunction is a leading cause of frailty and disability in the elderly (8). At the histological level, aging of gastrocnemius muscle in mice is characterized by muscle cell atrophy, variations in size of muscle fibers, presence of lipofuscin deposits, collagen deposition, and mitochondrial abnormalities (9).

A comparison of gastrocnemius muscle from 5-month (adult) and 30-month (old) mice (10–12) revealed that aging is associated with alterations in mRNA levels, which may reflect changes in gene expression, mRNA stability, or both. Of the 6347 genes surveyed in the oligonucleotide microarray, only 58 (0.9%) displayed a greater than twofold increase in expression levels as a function of age, whereas 55 (0.9%) displayed a greater than twofold decrease in expression. These findings are in agreement with a differential display analysis of gene expression in tissues of aging mice (13). Thus, the aging process is unlikely to be due to large, widespread alterations in gene expression.

Functional classes were assigned to genes displaying the largest alterations in expression (Table 1). Of the 58 genes that increased in expression with age, 16% were mediators of stress responses, including the heat shock factors Hsp71 and Hsp27, protease Do, and the DNA damage-inducible gene GADD45 (14). The largest differential expression between adult and aged animals (a 3.8-fold induction) was observed for the gene encoding the mitochondrial sarcomeric creatine kinase, a critical target for ROS-induced inactivation (15).

A consequence of skeletal muscle aging is loss of motor neurons followed by reinnervation of muscle fibers by the remaining intact neuronal units (16). Genes involved in neuronal growth accounted for 9% of genes highly induced in 30-month-old animals, including neurotrophin-3 (17), a growth factor induced during reinnervation, and synaptic vesicle protein-2, implicated in neurite extension (18). PEA3, a transcriptional factor induced in the response to

¹Environmental Toxicology Center, ²Institute on Aging, ³Departments of Genetics and Medical Genetics, University of Wisconsin, Madison, WI 53706, USA. ⁴Department of Medicine and Wisconsin Regional Primate Research Center, University of Wisconsin, Madison, WI and Veterans Administration Hospital, Geriatric Research, Education and Clinical Center, Madison, WI 53705, USA.

*To whom correspondence should be addressed at Department of Medicine, VA Hospital (GRECC 4D), 2500 Overlook Terrace, Madison, WI 53705, USA. E-mail: rhweindr@facstaff.wisc.edu (R.W.); Departments of Genetics and Medical Genetics, 445 Henry Mall, University of Wisconsin, Madison, WI 53706, USA. E-mail: taprolla@facstaff.wisc.edu (T.A.P.)

muscle injury and previously shown to be highly expressed in muscle from old rats (19), was also induced in aged muscle. We also observed parallels between our results and data from fibroblasts undergoing in vitro replicative senescence. For example, HIC-5, a transcriptional factor induced by oxidative damage, and insulin-like growth factor binding protein, both associated with in vitro senescence (20), are induced in aged skeletal muscle.

Fifty-five (0.9%) genes displayed a greater than twofold age-related decrease in expression. Genes involved in energy metabolism accounted for 13% of these alterations (Table 1). These include alterations in genes associated with mitochondrial function and turnover, such as the adenosine 5'-triphosphate (ATP) synthase A chain and nicotinamide adenine dinucleotide phosphate (NADP) transhydrogenase genes (both involved in mitochondrial bioenergetics), the LON protease implicated in mito-

chondrial biogenesis, and the ERV1 gene involved in mitochondrial DNA (mtDNA) maintenance (21). Additionally, a decrease in metabolic activity is suggested through a decline in the expression of genes involved in glycolysis, glycogen metabolism, and the glycerophosphate shunt (Table 1).

Aging was also characterized by large reductions (twofold or more) in the expression of biosynthetic enzymes such as squalene synthase (fatty acid and cholesterol synthesis), stearoyl-coenzyme A (CoA) desaturase (polyunsaturated fatty acid synthesis), and EF-1-gamma (protein synthesis). This suppression was accompanied by a concerted decrease in the expression of genes involved in protein turnover, such as the 20S proteasome subunit, the 26S proteasome component TBP1, ubiquitin-thiolesterase, and the Unp ubiquitin-specific protease, all of which are involved in the ubiquitin-proteasome pathway of protein turn-

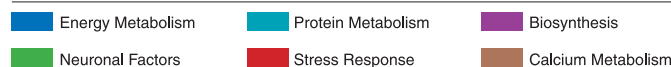
over (22). The directions of changes in other functional categories, such as signal transduction, and transcriptional and growth factors, did not present a consistent age-related trend.

In order to study the effects of CR on the gene expression profile of aging, we reduced caloric intake of C57BL/6 mice to 76% of that fed to control animals in early adulthood (2 months of age), and this dietary regimen was maintained until animals were killed at 30 months. A comparison of 30-month-old control and CR mice revealed that aging-related changes in gene expression profiles were remarkably attenuated by CR. Of the largest age-associated alterations (twofold or higher), 29% were completely prevented by CR and 34% were partially suppressed (Table 1). Of the four major gene classes that displayed consistent age-associated alterations, 84% were either completely or partially suppressed by CR. Thus, at the molecular level,

Table 1 (left). Aging-related changes in gene expression in gastrocnemius muscle. The extent to which caloric restriction prevented age-associated alterations in gene expression is denoted as either C (complete, >90%), N (none), or partial (20 to 90%, percentage effect indicated). The fold increase shown represents the average of all nine possible pairwise comparisons among individual mice determined by means of a specific algorithm (12). GenBank accession numbers are listed under ORF. A more comprehensive list that includes genes

that did not fit into the six classes can be found at www1.genetics.wisc.edu/prolla/Prolla_Tables.html. **Table 2 (right).** Caloric restriction-induced alterations in gene expression. The data represent a comparison between 30-month-old CR-fed and control-fed mice. The gene expression alterations listed in this Table are diet related and do not include those representing prevention of age-associated changes (see Table 1). Additional CR-induced changes are posted at the aforementioned Web site.

ORF	Δ Age (fold)	Gene	Function	CR Prevention
W08057	↑ 3.5	Heat Shock 27 kDa Protein	Chaperone	C
M17790	↑ 3.5	Serum Amyloid A Isoform 4	Unknown	N
AA114576	↑ 3.4	Heat Shock 71 kDa Protein	Chaperone	C
L28177	↑ 2.6	GADD45	DNA damage response	77%
M74570	↑ 2.4	Aldehyde Dehydrogenase II	Aldehyde detoxification	29%
AA059662	↑ 2.2	Protease Do Precursor	Protease	C
L22482	↑ 2.2	HIC-5	Senescence and differentiation	C
X99963	↑ 2.2	rhoB	Unknown	87%
X65627	↑ 2.1	TN22	RNA metabolism	64%
X57277	↑ 1.8	Rac1	JNK activator	C
AA071777	↑ 3.8	Synaptic Vesicle Protein 2	Neurite extension	51%
X53257	↑ 2.5	Neurotrophin-3	Reinnervation of muscle	50%
X78197	↑ 2.2	AP-2 Beta	Neurogenesis	N
X89749	↑ 2.1	mTGF	Differentiation	C
AA014024	↑ 2.1	Dynactin	Transport	55%
X63190	↑ 2.1	PEA3	Response to muscle injury	C
AA106112	↑ 3.8	Mitochondrial Sarcomeric Creatine Kinase	ATP generation	C
AA061886	↑ 2.0	Dihydropyridine-sensitive L-type Calcium Channel	Calcium channel	67%
AA061310	↓ 4.1	Mitochondrial LON Protease	Mitochondrial biogenesis	C
W55037	↓ 2.9	Alpha Enolase	Glycolysis	68%
V00719	↓ 2.6	Alpha-Amylase-1	Carbohydrate metabolism	N
M81475	↓ 2.5	Phosphoprotein Phosphatase	Glycogen metabolism	C
AA034842	↓ 2.1	ERV1	mtDNA maintenance	46%
AA106406	↓ 2.0	ATP Synthase A Chain	ATP synthesis	N
AA041826	↓ 2.0	IPP-2	Glycogen metabolism	C
L27842	↓ 2.0	PMP35	Peroxisome assembly	60%
Z49204	↓ 2.0	NADP Transhydrogenase	Glycerophosphate shunt	N
AA071776	↓ 1.9	Glucose-6-Phosphate Isomerase	Glycolysis	C
M13366	↓ 1.9	Glycerophosphate Dehydrogenase	Glycerophosphate shunt	C
AA107752	↓ 2.9	EF-1-Gamma	Protein synthesis	63%
U22031	↓ 2.6	20S Proteasome Subunit	Protein turnover	44%
AA061604	↓ 2.2	Ubiquitin Thiolesterase	Protein turnover	C
AA145829	↓ 2.1	26S Proteasome Component TBP1	Protein turnover	C
L00681	↓ 2.1	Unp Ubiquitin Specific Protease	Protein turnover	N
U35741	↓ 2.0	Rhodanese	Mitochondrial protein folding	C
D83585	↓ 1.7	Proteasome Z Subunit	Protein turnover	C
D76440	↓ 2.9	Necdin	Neuronal growth suppressor	47%
X75014	↓ 2.7	Phox2 Homeodomain Protein	Throphic factor	65%
M32240	↓ 2.1	GAS3	Myelin protein	55%
M16465	↓ 3.4	Calpactin I Light Chain	Calcium effector	C
L34611	↓ 2.3	PTHR	Calcium homeostasis	N
AA103356	↓ 2.2	Calmodulin	Calcium effector	N
D29016	↓ 6.4	Squalene Synthase	Cholesterol/fatty acid synthesis	52%
M21285	↓ 2.1	Stearoyl-CoA Desaturase	PUFA synthesis	C
U73744	↓ 2.1	HSP70	Chaperone	N



ORF	Δ CR (fold)	Gene	Function
U05809	↑ 4.5	Transketolase	Pentose phosphate pathway
W53351	↑ 4.1	Fructose-bisphosphate Aldolase	Glycolysis/Gluconeogenesis
AA071776	↑ 3.5	Glucose-6-Phosphate Isomerase	Glycolysis/Gluconeogenesis
U34295	↑ 2.3	Glucose Dependent Insulinotropic Polypeptide	Insulin sensitizer
U01841	↑ 2.3	Peroxisome Proliferator Receptor Gamma	Insulin sensitizer
L28116	↑ 2.0	PPAR Delta	Peroxisome induction
D42083	↑ 1.9	Fructose 1,6-bisphosphatase	Gluconeogenesis
AA041826	↑ 1.9	Protein Phosphatase Inhibitor 2 (IPP-2)	Inhibition of glycogen synthesis
U37091	↑ 1.8	Carbonic Anhydrase IV	CO ₂ disposal
M13366	↑ 1.8	Glycerophosphate Dehydrogenase	Electron transport to mitochondria
AA119868	↑ 1.7	Pyruvate Kinase	Glycolysis
AA145829	↑ 2.3	26S Protease Subunit TBP-1	Protein turnover
AA107752	↑ 2.2	Elongation Factor 1-gamma	Protein synthesis
W53731	↑ 2.1	Signal Recognition Receptor Alpha Subunit	Protein synthesis
U60328	↑ 2.1	Proteasome Activator PA28 Alpha Subunit	Protein turnover
X59990	↑ 2.0	mCyp-S1 (Cytochrome P450)	Protein folding
W08293	↑ 1.9	Translocin-Associated Protein Delta	Protein translocation
W57495	↑ 1.8	60S Ribosomal Protein L23	Protein synthesis
X13135	↑ 4.7	Fatty Acid Synthase	Fatty acid synthesis
X16314	↑ 2.5	Glutamine Synthetase	Glutamine synthesis
AA137659	↑ 2.4	Cytochrome P450-IIIC12	Steroid biosynthesis
L32973	↑ 2.0	Thymidylate Kinase	dTTP synthesis
X56548	↑ 2.0	Purine Nucleoside Phosphorylase	Purine turnover
AA022083	↑ 2.0	Huntingtin	Unknown
D76440	↑ 1.9	Necdin	Growth suppressor
AA062328	↓ 3.4	DnaJ Homolog 2	Chaperone
X63023	↓ 1.9	Cytochrome P-450-IIIa	Detoxification
U03283	↓ 1.8	Cyp1b1 Cytochrome P450	Detoxification
U14390	↓ 1.8	Aldehyde Dehydrogenase-3	Detoxification
X76850	↓ 1.8	MAPKAP2	Unknown
D26123	↓ 1.7	Carbonyl Reductase	Detoxification
L4406	↓ 1.7	Hsp105-beta	Chaperone
U40930	↓ 1.5	Oxidative Stress-Induced Protein	Unknown
U66887	↓ 1.8	RAD50	Double strand break repair
AA059718	↓ 1.7	DNA Polymerase Beta	Base excision repair
W42234	↓ 1.6	XPE	Nucleotide excision repair
D43694	↓ 1.8	Meth-1	Differentiation
D16464	↓ 1.7	HES-1	Differentiation
W13191	↓ 1.6	Thyroid Hormone Receptor Alpha-2	Thyroid hormone receptor



CR mice appear to be biologically younger than animals receiving the control diet.

Caloric restriction induced a metabolic reprogramming characterized by a transcriptional shift toward energy metabolism, increased biosynthesis, and protein turnover (Table 2). CR resulted in the induction of 51 genes (1.8-fold or higher) as compared with age-matched animals consuming the control diet. Nineteen percent of genes in this class are related to energy metabolism. Modulation of energy metabolism was evident through the induction of glucose-6-phosphate isomerase (glycolysis), fructose 1,6-bisphosphatase (gluconeogenesis), IPP-2 (an inhibitor of glycogen synthesis), and transketolase. Fructose 1,6-bisphosphatase switches the direction of a key regulatory step in glycolysis toward a biosynthetic precursor, glucose-6-phosphate. Remarkably, this same adaptation has been observed as part of the transcriptional reprogramming of *Saccharomyces cerevisiae* accompanying the diauxic switch from anaerobic growth to aerobic respiration upon depletion of glucose (23). Transketolase, which controls the nonoxidative branch of the pentose phosphate pathway, provides NADPH for biosynthesis and reducing power for several antioxidant systems. CR also induced transcripts associated with fatty acid metabolism, such as fatty acid synthase and PPAR- δ , a mediator of peroxisome proliferation. Interestingly, CR may act to increase insulin sensitivity through the induction of glucose-dependent insulinotropic peptide and PPAR- γ , a potent insulin sensitizer (24).

Biosynthetic ability also appears to be induced in CR mice. CR up-regulated the expression of glutamine synthase, purine nucleoside phosphorylase (purine turnover), and thymidylate kinase (dTTP synthesis). Remarkably, 16% of transcripts highly induced by CR encode proteins involved in protein synthesis and turnover, including elongation factor 1- γ , proteasome activator PA28,

translocon-associated protein delta, 60S ribosomal protein L23, and the 26S proteasome subunit TBP-1.

CR was associated with a 1.6-fold or greater reduction in expression of 57 genes. Of these, 12% were associated with stress responses or DNA repair pathways, or both (Table 2). Among the 6347 genes examined, the most substantial suppression of gene expression by CR was for a murine DnaJ homolog (3.4-fold), a pivotal and inducible heat shock factor that senses and transduces the presence of misfolded or damaged proteins in bacteria (25). CR also lowered the expression of cytochrome P450 isoforms IIIA and Cyp1b1 (involved in detoxification), Hsp105 (a heat shock factor), aldehyde dehydrogenase (an inducible enzyme involved in detoxification of metabolic by-products), and an oxidative stress-induced protein of unknown function. CR reduced the expression of several DNA repair genes including XPE (a factor that recognizes multiple DNA adducts), RAD50 (involved in double-strand break repair), and DNA polymerase- β (a DNA damage-inducible polymerase). We also find molecular evidence to support a state of lower basal metabolic rate in CR mice through lowered expression of the thyroid-hormone receptor alpha gene (26).

The data presented here provide the first global assessment of the aging process in mammals at the molecular level and underscore the utility of large-scale, parallel gene expression analysis in the study of complex biological phenomena. We estimate that the 6347 genes analyzed in this study represent 5 to 10% of the mouse genome. Additional classes of aging-related genes in skeletal muscle may be discovered with the development of higher density mammalian DNA microarrays. The observed collection of gene expression alterations in aging skeletal muscle is complex, reflecting the presence of myocyte, neuronal, and vascular components. Although some of the age-associated alterations in gene

expression could represent maturational changes, this possibility is unlikely given the fact that the 5-month-old (adult) mice used in this study were fully mature animals. Importantly, changes in mRNA levels may not always result in a parallel alteration in protein levels. However, the complete or partial prevention of most age-related alterations by CR suggests that gene expression profiles can be used to assess the biological age of mammalian tissues, providing a tool for evaluating experimental interventions.

Taken as a whole, our results provide evidence that during aging there is an induction of a stress response as a result of damaged proteins and other macromolecules. This response ensues as the systems required for the turnover of such molecules decline, perhaps as a result of an energetic deficit in the cell. In particular, the observed alterations in transcripts associated with energy metabolism and mitochondrial function may reflect either decreased mitochondrial biogenesis or turnover secondary to cumulative ROS-inflicted mitochondrial damage (2), lending support to the concept that mitochondrial dysfunction plays a central role in aging of postmitotic tissues. The gene expression profile also suggests that secondary responses to the aging process in skeletal muscle involve the activation of neuronal and myogenic responses to injury.

A summary of global changes induced by aging, and the contrasting effects of CR, are shown in Table 3. The transcriptional activation of stress response genes that process damaged or misfolded proteins during aging, and the prevention of this induction by CR, suggest a central role for protein modifications in aging. Indeed, aging is characterized by an exponential increase of oxidatively damaged proteins (27). Previous analyses of metabolic rates in CR animals have led to the suggestion that this life-extending regimen acts through a reduction in metabolic rate, resulting in a lower production of toxic by-products of metabolism (28). The CR-mediated reduction of mRNAs encoding inducible genes involved in metabolic detoxification, DNA repair, and the response to oxidative stress supports this view, because it implies lower substrate availability for these systems. Additionally, our analysis indicates that CR may cause a metabolic shift toward increased biosynthesis and macromolecular turnover. A hormonal trigger for this shift may be an alteration in the insulin signaling pathway through increased expression of genes that mediate insulin sensitivity, a finding that links our observations to those obtained through the genetic analysis of aging in the nematode *C. elegans* (4).

References and Notes

1. S. M. Jazwinski, *Science* **273**, 54 (1996); G. M. Martin, S. N. Austad, T. E. Johnson, *Nature Genet.* **13**, 25 (1996); F. B. Johnson, D. A. Sinclair, L. Guarente, *Cell* **96**, 291 (1996).

Table 3. Global view of transcriptional changes induced by aging and caloric restriction.

Aging	Caloric restriction
↑ Stress response Induction of: Heat shock response DNA damage-inducible genes Oxidative stress-inducible genes	↑ Protein metabolism Increased synthesis Increased turnover
↓ Energy metabolism Reduced glycolysis Mitochondrial dysfunction	↑ Energy metabolism Up-regulation of gluconeogenesis, and the pentose phosphate shunt
↑ Neuronal injury Reinnervation Neurite extension and sprouting	↑ Biosynthesis Fatty acid synthesis Nucleotide precursors
	↓ Macromolecular damage Suppression of: Inducible heat shock factors Inducible detoxification systems Inducible DNA repair systems

2. K. B. Beckman and B. N. Ames, *Physiol. Rev.* **78**, 547 (1998).
3. W. C. Orr and R. S. Sohal, *Science* **263**, 1128 (1994); T. L. Parkes et al., *Nature Genet.* **19**, 171 (1998).
4. S. Ogg et al., *Nature* **389**, 994 (1997); K. Lin, J. B. Dorman, A. Rodan, C. Kenyon, *Science* **278**, 1319 (1997); S. Paradis and G. Ruvkun, *Genes Dev.* **12**, 2488 (1998); H. A. Tissenbaum and G. Ruvkun, *Genetics* **148**, 703 (1998).
5. T. E. Johnson, *Science* **249**, 908 (1990); S. Murakami and T. E. Johnson, *Genetics* **143**, 1207 (1996); Y.-J. Lin, L. Seroude, S. Benzer, *Science* **282**, 943 (1998).
6. C. E. Yu et al., *Science* **272**, 258 (1996); L. Ye et al., *Am. J. Med. Genet.* **68**, 494 (1997).
7. R. Weindruch and R. L. Walford, *The Retardation of Aging and Disease by Dietary Restriction* (Thomas, Springfield, IL, 1988).
8. C. Dutta, E. C. Hadley, J. Lexell, *Muscle Nerve* **5**, S5 (1997).
9. R. Ludatscher, M. Silberman, D. Gershon, A. Reznick, *Exp. Gerontol.* **18**, 113 (1983).
10. Methods used to house and feed male C57BL/6 mice, a commonly used model in aging research with an average life-span of ~30 months, were recently described [T. D. Pugh, T. D. Oberley, R. Weindruch, *Cancer Res.* **59**, 642 (1999)].
11. Total RNA was extracted from frozen tissue by using TRIzol reagent (Life Technologies). Polyadenylate [poly(A)⁺] RNA was purified from the total RNA with oligo-dT-linked Oligotex resin (Qiagen). One microgram of poly(A)⁺ RNA was converted into double-stranded cDNA (ds-cDNA) by using SuperScript Choice System (Life Technologies) with an oligo-dT primer containing a T7 RNA polymerase promoter (Genset). After second-strand synthesis, the reaction mixture was extracted with phenol-chloroform-isoamyl alcohol, and ds-cDNA was recovered by ethanol precipitation. In vitro transcription was performed by using a T7 Megascript Kit (Ambion) with 1.5 µl of ds-cDNA template in the presence of a mixture of unlabeled ATP, CTP, GTP, and UTP and biotin-labeled CTP and UTP [bio-11-CTP and bio-16-UTP (Enzo)]. Biotin-labeled cRNA was purified by using an RNeasy affinity column (Qiagen), and fragmented randomly to sizes ranging from 35 to 200 bases by incubating at 94°C for 35 min. The hybridization solutions contained 100 mM MES, 1 M Na⁺, 20 mM EDTA, and 0.01% Tween 20. The final concentration of fragmented cRNA was 0.05 µg/µl in the hybridization solutions. After hybridization, the hybridization solutions were removed and the gene chips were washed and stained with streptavidin-phycoerythrin. DNA chips were read at a resolution of 6 µm with a Hewlett-Packard GeneArray Scanner.
12. Detailed protocols for data analysis of Affymetrix microarrays and extensive documentation of the sensitivity and quantitative aspects of the method have been described [D. J. Lockhart, *Nature Biotechnol.* **14**, 1675 (1996)]. Briefly, each gene is represented by the use of ~20 perfectly matched (PM) and mismatched (MM) control probes. The MM probes act as specificity controls that allow the direct subtraction of both background and cross-hybridization signals. The number of instances in which the PM hybridization signal is larger than the MM signal is computed along with the average of the logarithm of the PM:MM ratio (after background subtraction) for each probe set. These values are used to make a matrix-based decision concerning the presence or absence of an RNA molecule. Positive average signal intensities after background subtraction were observed for over 4000 genes for all samples. To determine the quantitative RNA abundance, the average of the differences representing PM minus MM for each gene-specific probe family is calculated, after discarding the maximum, the minimum, and any outliers beyond 3 SDs. Averages of pairwise comparisons were made between animals with Affymetrix software. To determine the effect of age, each 5-month-old mouse (*n* = 3) was compared to each 30-month-old (*n* = 3) mouse, generating a total of nine pairwise comparisons. To determine the effect of diet, 30-month-old CR-fed (*n* = 3) and 30-month-old control-fed (*n* = 3) animals were similarly compared. Pearson correlation coefficients were calculated between individual animals in the same age/diet groups. No correlation coefficient between two animals in the same age/diet group was less than 0.98.
13. M. H. Goyns et al., *Mech. Ageing Dev.* **101**, 73 (1998).
14. J. Jackman, I. Alamo Jr., A. J. Fornace Jr., *Cancer Res.* **54**, 5656 (1994).
15. O. Stachowiak, M. Dolder, T. Wallimann, C. Richter, *J. Biol. Chem.* **273**, 16694 (1998).
16. L. Larsson, *J. Gerontol. Biol. Sci.* **50A**, 96 (1995); J. Lexell, *J. Nutr.* **127**, 1011S (1997).
17. J. C. Copray and N. Brouwer, *Neurosci. Lett.* **236**, 41 (1997).
18. G. Marazzi and K. M. Buckley, *Dev. Dyn.* **197**, 115 (1993).
19. C. A. Peterson and J. D. Houle, *J. Nutr.* **127**, 1007S (1997).
20. M. Shibamura, J. Mashimo, T. Kuroki, K. Nose, *J. Biol. Chem.* **269**, 26767 (1994); S. Wang, E. J. Moerman, R. A. Jones, R. Thweatt, S. Goldstein, *Mech. Ageing Dev.* **92**, 121 (1996).
21. ATP synthase: W. Junge, H. Lill, S. Engelbrecht, *Trends Biochem. Sci.* **22**, 420 (1997); NADP transhydrogenase: J. B. Hoek and J. Rydstrom, *Biochem. J.* **254**, 1 (1988); LON protease: K. Luciakova, B. Sokolikova, M. Chloupkova, B. D. Nelson, *FEBS Lett.* **444**, 186 (1999); ERV1: T. Lisowsky, *Curr. Genet.* **26**, 15 (1994).
22. A. L. Schwartz and A. Ciechanover, *Annu. Rev. Med.* **50**, 57 (1999).
23. J. L. DeRisi, V. R. Iyer, P. O. Brown, *Science* **278**, 680 (1997).
24. J. R. Zierath et al., *Endocrinology* **139**, 5034 (1998).
25. T. Tomoyasu, T. Ogura, T. Tatsuta, B. Bukau, *Mol. Microbiol.* **30**, 567 (1998); T. Yura, H. Nagai, H. Mori, *Annu. Rev. Microbiol.* **47**, 321 (1993).
26. L. Wikstrom et al., *EMBO J.* **17**, 455 (1998).
27. E. R. Stadtman, *Science* **257**, 1220 (1992).
28. R. S. Sohal and R. Weindruch, *ibid.* **273**, 59 (1996).
29. Supported by NIH grants PO1 AG11915 (R.W.) and RO1 CA78723 (T.A.P.). T.A.P. is a recipient of the Shaw Scientist (Milwaukee Foundation) and Burroughs Wellcome Young Investigator awards.

19 May 1999; accepted 22 July 1999

Dual Function of the Selenoprotein PHGPx During Sperm Maturation

Fulvio Ursini,¹ Sabina Heim,² Michael Kiess,² Matilde Maiorino,¹ Antonella Roveri,¹ Josef Wissing,² Leopold Flohé^{3*}

The selenoprotein phospholipid hydroperoxide glutathione peroxidase (PHGPx) changes its physical characteristics and biological functions during sperm maturation. PHGPx exists as a soluble peroxidase in spermatids but persists in mature spermatozoa as an enzymatically inactive, oxidatively cross-linked, insoluble protein. In the midpiece of mature spermatozoa, PHGPx protein represents at least 50 percent of the capsule material that embeds the helix of mitochondria. The role of PHGPx as a structural protein may explain the mechanical instability of the mitochondrial midpiece that is observed in selenium deficiency.

Selenium is essential for male fertility in rodents and has also been implicated in the fertilization capacity of spermatozoa of livestock and humans (1). Selenium deficiency is associated with impaired sperm motility, structural alterations of the midpiece, and loss of flagellum (1). However, three decades after the discovery of selenium as an integral constituent of redox enzymes (2), the molecular basis of the relationship of the essential trace element and male fertility remains obscure. The selenoprotein PHGPx (Enzyme Commission number 1.11.1.12) is abundantly expressed in spermatids and displays high activity in postpubertal testis (3). In mature spermatozoa, however, selenium is largely restricted to the mitochondrial capsule, a keratin-like matrix that embeds the

helix of mitochondria in the sperm midpiece (4). A "sperm mitochondria-associated cysteine-rich protein (SMCP)" (5) had been considered to be the selenoprotein accounting for the selenium content of the mitochondrial capsule (4–6). The rat SMCP gene, however, does not contain an in-frame TGA codon (7) that would enable a selenocysteine incorporation (8). In mice, the three in-frame TGA codons of the SMCP gene are upstream of the translation start (5). SMCP can therefore no longer be considered as a selenoprotein. Instead, the "mitochondrial capsule selenoprotein (MCS)," as SMCP was originally referred to (4–7), is here identified as PHGPx.

Routine preparations of rat sperm mitochondrial capsules (9) yielded a fraction that was insoluble in 1% SDS containing 0.2 mM dithiothreitol (DTT) and displayed a vesicular appearance in electron microscopy (Fig. 1A). The vesicles readily disintegrated upon exposure to 0.1 M mercaptoethanol (Fig. 1B) and became fully soluble in 6 M guanidine-HCl. When the solubilized capsule material was subjected to polyacrylamide gel electrophoresis (PAGE), four bands in the 20-kD

¹Dipartimento di Chimica Biologica, Università di Padova, Viale G. Colombo 3, I-35121 Padova, Italy.

²National Research Centre for Biotechnology (GBF), Mascheroder Weg 1, D-38124 Braunschweig, Germany.

³Department of Biochemistry, Technical University of Braunschweig, Mascheroder Weg 1, D-38124 Braunschweig, Germany.

*To whom correspondence should be addressed. E-mail: lfl@gbf.de